THE JOURNAL OF PHYSICAL CHEMISTRY LETTERS
A JOURNAL OF THE AMERICAN CHEMICAL SOCIETY

pubs.acs.org/JPCL

Letter

Simulating Cavity-Modified Electron Transfer Dynamics on NISQ Computers

Ningyi Lyu, Pouya Khazaei, Eitan Geva,* and Victor S. Batista*

Cite This: *J. Phys. Chem. Lett.* 2024, 15, 9535−9542

Read Online

ACCESS | Metrics & More | Article Recommendations

ABSTRACT: We present an algorithm based on the quantum-mechanically exact tensor-train thermo-field dynamics (TT-TFD) method for simulating cavity-modified electron transfer dynamics on noisy intermediate-scale quantum (NISQ) computers. The utility and accuracy of the proposed methodology is demonstrated on a model for the photoinduced intramolecular electron transfer reaction within the carotenoid−porphyrin−C_{60} molecular triad in tetrahydrofuran (THF) solution. The electron transfer rate is found to increase significantly with increasing coupling strength between the molecular system and the cavity. The rate process is also seen to shift from overdamped monotonic decay to underdamped oscillatory dynamics. The electron transfer rate is seen to be highly sensitive to the cavity frequency, with the emergence of a resonance cavity frequency for which the effect of coupling to the cavity is maximal. Finally, an implementation of the algorithm on the IBM Osaka quantum computer is used to demonstrate how TT-TFD-based electron transfer dynamics can be simulated accurately on NISQ computers.

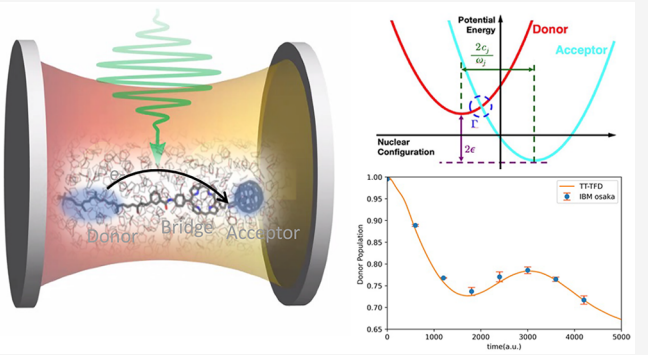

Exploring the potential of light-matter interactions to influence chemical reactions has captivated the attention of physical chemists for many years.[1−11] Recent experimental advancements showcased the possibility of utilizing these interactions to control various chemical and physical phenomena, including electronic energy and charge transfer, chemical reactions and photocatalysis.[12−68] The proposed mechanisms for those observations often invoke strong coupling between the optical cavity modes and the electronic and vibrational degrees of freedom (DOF) of molecules placed within these cavities.

These experimental advances call for the development of accurate computational methods for simulating the dynamics of molecular matter inside cavities, toward revealing the fundamental mechanisms underlying them and predicting the effect on reaction yields and rates. So far, most dynamical simulations have been based on classical, semiclassical, quasiclasscial and mixed quantum classical (MQC) methods, which might not describe quantum effects properly within the part of the system which is treated as classical-like.[49,69−77] An attractive alternative is offered by recently developed quantum-mechanically exact numerical methods that are applicable to systems with a few tens to a few hundreds nuclear and photonic DOF.[78−83] Implementing those methods on quantum computing platforms[84−90] can further extend their range of applicability to even more complex chemical systems, which would be necessary for bridging the gap between simulation and experiment.

In this work, we report results obtained by using the tensor-train thermo-field dynamics (TT-TFD) method[91−93] to perform a quantum-mechanically exact simulation of the electron transfer dynamics within a molecular system confined within an optical cavity. Utilizing our recently proposed scheme based on the Sz.-Nagy dilation protocol[94,95] for the purpose of simulating nonunitary open quantum dynamics on quantum computers,[96,97] we also propose and implement an algorithm for simulating the aforementioned quantum dynamics on currently available IBM Noisy Intermediate-Scale Quantum (NISQ) computers.

For the sake of concreteness, we showcase the methodology in the context of a model designed to capture the essential physics underlying photoinduced intramolecular electron transfer in a carotenoid−porphyrin−C_{60} molecular triad dissolved in liquid tetrahydrofuran (THF) (see Figure 1). To this end, we investigate the effect on intramolecular

Received: July 28, 2024
Revised: September 7, 2024
Accepted: September 9, 2024

https://doi.org/10.1021/acs.jpclett.4c02220
J. Phys. Chem. Lett. 2024, 15, 9535−9542

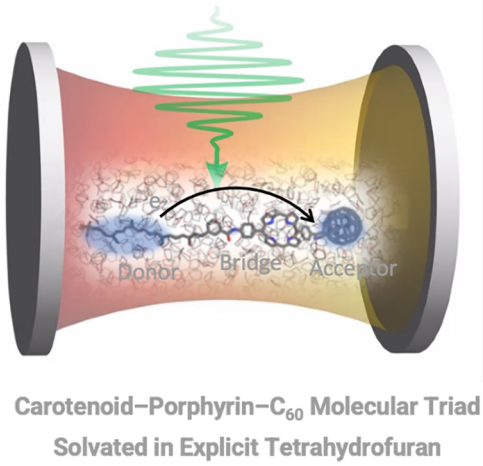

Figure 1. Illustration of the THF-solvated carotenoid–porphyrin–C_{60} molecular triad in cavity. Adapted with the permission from ref 101. Copyright 2024 AIP Publishing.

electron transfer dynamics of placing the molecular system inside a lossless optical cavity. While it would be desirable to consider the effect of cavity losses on the cavity-modified charge transfer rates, particularly for studies that might aim to provide comparisons to data from specific experiments, our study employs a lossless cavity to enable direct comparisons to an extended literature of recent studies focused on models that neglect the effects of the cavity finite lifetime, as outlined in the review article by Mandal et al.[63] Furthermore, we quote from the same review article that studies investigated the effect of cavity loss have found that "while cavity loss may sometimes be a hindrance to enhancing reactivity on polaritonic surfaces, it may also serve to improve the desired reactivity and even act as another tunable knob to control photochemical reactivity".[63] Therefore, the effect of cavity loss is system dependent. The lossless cavity model investigated allows us to make meaningful comparisons to earlier simulations that employed the same lossless cavity model as in a recent paper demonstrating the utility of RPMD for calculating cavity modified rates,[98] and three recent papers that demonstrate the utility of LSC-based methods for calculating cavity modified rates[51] and to develop a theory for cavity-modified FGR and Marcus theory charge transfer rate constants.[99,100] Therefore, the model of a lossless cavity is ideally suited to demonstrate the usefulness of TT-TFD to calculate cavity-modified charge transfer rates on NISQ computers as directly compared to recent theoretical studies. We find that the dynamics can be significantly modified by changing the frequency of the cavity, as well as the strength of the light-matter interaction. Our numerically exact results are also compared to calculations based on the approximate ring-polymer molecular dynamics (RPMD) methodology,[49] and showed that it provides qualitatively reliable ultrafast population dynamics for the studied model system.

We consider the following Hamiltonian of a molecular system capable of undergoing an electron transfer reaction while being coupled to a lossless optical cavity:

$$\hat{H} = -\epsilon|A\rangle\langle A| + \Delta(|D\rangle\langle A| + |A\rangle\langle D|) + \hat{H}_B + \hat{H}_F \tag{1}$$

In the contest of this study, $|D\rangle$ and $|A\rangle$ denote the $\pi\pi^*$ and CT1 diabatic states of the solvated triad, respectively, $-\epsilon = -532$ meV is the reaction free energy and $\Delta = 24$ meV is the electronic coupling coefficient.[102] $\hat{H}_B$ describes the bath, while $\hat{H}_F$ describes cavity-molecule coupling.

The bath Hamiltonian $\hat{H}_B$, is given in terms of the mass-weighted bath coordinates and momenta $\{\hat{R}_j, \hat{P}_j\}$, associated with the corresponding set of nuclear harmonic modes:

$$\hat{H}_B = \sum_{j=1}^{50}\left(\frac{\hat{P}_j^2}{2} + \frac{\omega_j^2}{2}\hat{R}_j^2\right)|D\rangle\langle D| + \sum_{j=1}^{50}\left(\frac{\hat{P}_j^2}{2} + \frac{\omega_j^2}{2}\left(\hat{R}_j - \frac{c_j}{\omega_j^2}\right)^2\right)|A\rangle\langle A|$$

Here, the bath frequencies $\{\omega_j\}$ and coupling constants $\{c_j\}$ are obtained by discretizing the following Ohmic spectral density:

$$J(\omega) = \frac{\pi}{2}\sum_{j=1}^{50}\frac{c_j^2}{m_j\omega_j}\delta(\omega - \omega_j) = \eta\omega e^{-\omega/\omega_c} \tag{2}$$

where $\omega_c = 6.57$ meV, and $\eta = 1.066 \times 10^6$ au are chosen so that the discretized vibrational frequencies roughly cover the range of normal-mode frequencies for the carotenoid–porphyrin–C_{60}/THF system under consideration, as previously calculated by molecular dynamics simulations.[103]

The couplings $\{c_j\}$ are then scaled with a constant a, such that the values of the scaled $\tilde{c}_j = c_j a$ correspond to the calculated molecular reorganization energy for the triad molecule in the bent conformation, namely $\lambda = 515$ meV:[103]

$$\frac{1}{2}\sum_{j=1}^{50}\omega_j^2\tilde{c}_j^2 = \lambda \tag{3}$$

Finally, $\hat{H}_F$ describes the coupling of the optical cavity mode with the molecular system:

$$\hat{H}_F = \hbar\omega_p\hat{a}_p^\dagger\hat{a}_p + \hbar g_p(|D\rangle\langle A| + |A\rangle\langle D|)(\hat{a}_p^\dagger + \hat{a}_p) \tag{4}$$

Here, $\hat{a}_p$ and $\hat{a}_p^\dagger$ are the photonic annihilation and creation operators, respectively. The values of the light-matter coupling strength (g_p) and the cavity frequency (ω_p) determine the effect of the cavity and will be varied below to evaluate their effect on the electron transfer dynamics.

The time evolution of the density operator that describes the state of the overall system, $\hat{\rho}(t)$, is described by the quantum Liouville equation:

$$\frac{\mathrm{d}}{\mathrm{d}t}\hat{\rho}(t) = -\frac{i}{\hbar}[\hat{H}, \hat{\rho}(t)] \tag{5}$$

where $\hat{H}$ is as in eq 1. The TT-TFD method solves this equation in vectorized form, as follows:

$$\frac{\mathrm{d}}{\mathrm{d}t}|\psi(\beta, t)\rangle = -\frac{i}{\hbar}\bar{H}|\psi(\beta, t)\rangle \tag{6}$$

with $\bar{H} = \hat{H} \otimes \tilde{I}$. Here, $|\psi(\beta,t)\rangle$ is the thermal wave function from which the density operator $\hat{\rho}(t)$ can be obtained as follows:

$$\hat{\rho}(t) = \mathrm{Tr}_f\{|\psi(\beta, t)\rangle\langle\psi(\beta, t)|\} \tag{7}$$

with $\hat{\rho}(0)$ obtained from eq 7 with the initial thermal distribution:

https://doi.org/10.1021/acs.jpclett.4c02220
J. Phys. Chem. Lett. 2024, 15, 9535−9542

$$|\psi(0,\beta)\rangle = Z^{-1/2}\sum_n e^{-\beta E_n/2}|n,\tilde{n}\rangle \tag{8}$$

This transformation effectively recasts eq 5 into eq 6, which has the form of a time-dependent Schrödinger equation (TDSE) for the thermal wave function, $|\psi(\beta,t)\rangle$. Note that according to eq 8, the thermal wave function is defined in a double Hilbert space $\mathcal{H}\otimes\tilde{\mathcal{H}}$, including states $|\tilde{n}\rangle$ that are identical copies of states $|n\rangle$ in a Hilbert space $\tilde{\mathcal{H}}$ that is an exact copy of the physical Hilbert space $\mathcal{H}$.

The preparation of the initial state $|\psi(\beta,0)\rangle$ (see eq 8) requires imaginary time propagation, which could be computationally costly. However, when the bath Hamiltonian is harmonic, as is the case here, we can define the Hamiltonian, as follows:

$$\bar{H} = \hat{H}\otimes\tilde{I} - \hat{I}\otimes\sum_j \omega_j\tilde{a}_j^\dagger\tilde{a}_j \tag{9}$$

As a result, the aforementioned imaginary time propagation can be circumvented by utilizing the thermal Bogoliubov transformation:

$$|0(\beta)\rangle = e^{-i\hat{G}}|0,\tilde{0}\rangle \tag{10}$$

where

$$\hat{G} = -i\sum_j \theta_j(\hat{a}_j\tilde{a}_j - \hat{a}_j^\dagger\tilde{a}_j^\dagger) \tag{11}$$

with $\theta_j = arctanh(e^{-\beta\omega_j/2})$ and $\hat{a}_j$, $\hat{a}_j^\dagger$ ($\tilde{a}_j$, $\tilde{a}_j^\dagger$) the physical (fictional) bosonic creation and annihilation operators for the jth degree of freedom.

Substituting eqs 10 and 11 into eq 6, we obtain

$$\frac{d|\psi_\theta(\beta,t)\rangle}{dt} = -\frac{i}{\hbar}\bar{H}_\theta|\psi_\theta(\beta,t)\rangle \tag{12}$$

where:

$$\begin{aligned}\bar{H}_\theta &= e^{i\hat{G}}\bar{H}e^{-i\hat{G}}\\ |\psi_\theta(\beta,0)\rangle &= e^{i\hat{G}}|\psi(\beta,0)\rangle = |0,\tilde{0}\rangle\end{aligned} \tag{13}$$

For a system that involves many nuclear DOF, the thermal wavepacket is a high-dimensional tensor whose full representation faces the curse of dimensionality. The tensor train (TT) decomposition[81−83] is a numerically exact data compression strategy that allows one to cast a moderately entangled wave function in terms of a train of 2- or 3-dimensional tensors, such that they can be stored and computed efficiently. TT-TFD expresses $|0,\tilde{0}\rangle$ as a rank-1 tensor train, and propagates eq 12 to obtain $|\psi_\theta(\beta,t)\rangle$. The propagation can be carried out with the TT-KSL integrator.[92,93] The expectation value of physical observables $\hat{A}$ are obtained, as follows:

$$\langle A(t)\rangle = \langle\psi_\theta(\beta,t)|\bar{A}_\theta|\psi_\theta(\beta,t)\rangle \tag{14}$$

where $\bar{A}_\theta = e^{i\hat{G}}\bar{A}e^{-i\hat{G}}$ and $\bar{A} = \hat{A}\otimes\tilde{I}$.

Numerically exact TT-TFD simulations of the model carotenoid−porphyrin−C_{60}/THF molecular system confined to an optical cavity were performed based on the protocol outlined above. In the following, we describe the quantum computing procedure used for obtaining the time evolution of the electronic donor and acceptor states of the model system.

Our propagation scheme is based on the so-called population-only Liouville space propagator, $\mathcal{P}^{pop}(t)$, defined by

$$\hat{\sigma}^{pop}(t) = \mathcal{P}^{pop}(t)\hat{\sigma}^{pop}(0) \tag{15}$$

Here, $\hat{\sigma}(t) = \mathrm{Tr}_{np}[\hat{\rho}(t)]$ is the reduced electronic density operator, obtained by partially tracing $\hat{\rho}(t)$ over the nuclear/photonic Hilbert space (designated by Tr_{np}). Whereas $\hat{\sigma}(t)$ is represented by a 2×2 matrix whose diagonal and off-diagonal elements correspond to the donor and acceptor populations and off-diagonal elements correspond to the coherence between them, $\hat{\sigma}^{pop}(t) = (\sigma_{00}(t), \sigma_{11}(t))^T$ includes only the diagonal elements of $\hat{\sigma}(t)$, necessary for describing the electron transfer dynamics. The preparation of the superoperator $\mathcal{P}^{pop}(t)$ according to the TT-TFD generated population dynamics is described in Appendix E of ref 104.

To perform quantum electron transfer dynamics simulations based on eq 15, we first transform $\mathcal{P}^{pop}(t)$ into a unitary matrix using the Sz.-Nagy dilation theorem,[94] as follows:[95,105]

$$\mathcal{U}_{\mathcal{P}^{pop}}(t) = \begin{pmatrix}\mathcal{P}^{pop}(t) & \sqrt{I-\mathcal{P}^{pop}(t)\mathcal{P}^{pop^\dagger}(t)}\\ \sqrt{I-\mathcal{P}^{pop^\dagger}(t)\mathcal{P}^{pop}(t)} & -\mathcal{P}^{pop^\dagger}(t)\end{pmatrix} \tag{16}$$

The initial state is dilated by appending it with ancillary zero elements, as follows:

$$\begin{aligned}\hat{\sigma}^{pop}(0) &= (\sigma_{00}(0),\sigma_{11}(0))^T \rightarrow \tilde{\sigma}^{pop}(0)\\ &= (\sigma_{00}(0),\sigma_{11}(0),0,0)^T\end{aligned} \tag{17}$$

The dilated time-updated population-only density matrix is obtained, as follows:

$$\tilde{\sigma}^{pop}(t) = \mathcal{U}_{\mathcal{P}^{pop}}(t)\tilde{\sigma}^{pop}(0) \tag{18}$$

The dilation scheme thus provides the unitary matrix $\mathcal{U}_{\mathcal{P}^{pop}}(t)$ governing the time-evolution of $\tilde{\sigma}^{pop}(t)$, the first two elements of which coincide with the sought after donor and acceptor populations as a function of time, $\hat{\sigma}^{pop}(t)$. Therefore, eqs 18 and 15 describe the same dynamics, with eq 18 allowing for simulations on a NISQ quantum computer. For the two-state model under consideration, $\mathcal{U}_{\mathcal{P}^{pop}}(t)$ is a 4×4 unitary matrix that can be transpiled onto a quantum circuit given in terms of a sequence of 1-qubit and 2-qubit gates.

Figure 2 compares the time evolution of the donor population in the carotenoid−porphyrin−C_{60}/THF system under consideration at different values of g_p, with the cavity frequency ω_p held fixed at a value close to resonance (see below) and $g_p = 0$ corresponding to the cavity-free case. No significant electron transfer dynamics occurs on the ∼120 fs time scale shown in the cavity-free case, which is consistent with previously obtained estimates based on Fermi's golden rule (FGR), according to which cavity-free electron transfer rates for this system occurs on a picosecond time scale.[102] However, coupling to the cavity mode is seen to give rise to significant electron transfer dynamics on this time scale, which is highly sensitive to the values of g_p. More specifically, increasing g_p modifies the electron transfer dynamics qualitatively from overdamped monotonic decay to underdamped oscillatory dynamics. The fact that the frequency of the oscillations coincides with g_p implies that its appearance is a

https://doi.org/10.1021/acs.jpclett.4c02220
J. Phys. Chem. Lett. 2024, 15, 9535−9542

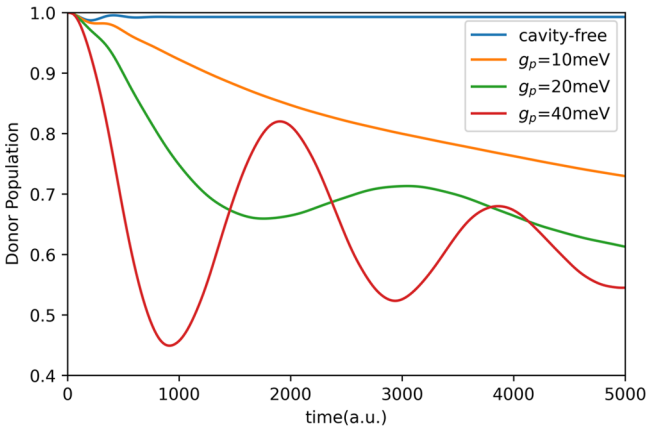

Figure 2. Time-dependent population of the ($\pi\pi^*$) donor state following the photoexcitation of the carotenoid−porphyrin−C_{60} molecular triad solvated in tetrahydrofuran (THF) prepared in a geometry relaxed bent configuration in an optical cavity. The cavity frequency is set as ω_p = 400 meV for all calculations, while the light−matter interaction strength is varied according to g_p = 10, 20, and 40 meV. The temperature is set at T = 300 K. The calculations are based on TT-TFD simulations with a propagation time-step τ = 1 *au*.

manifestation of the emergence of the strong field-matter coupling regime.

Figure 3 compares the time evolution of the donor population in the carotenoid−porphyrin−C_{60}/THF system

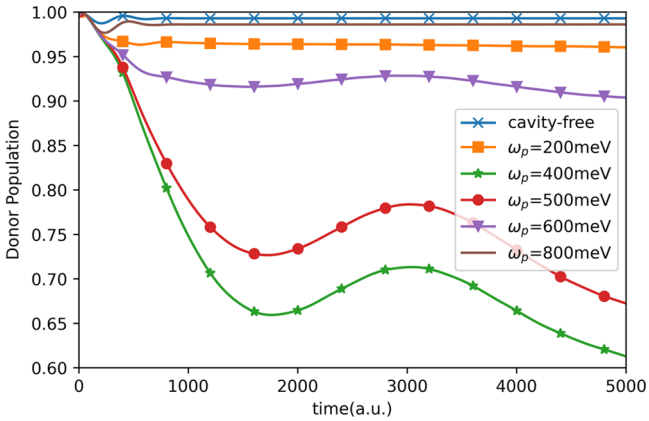

Figure 3. Time-dependent population of the ($\pi\pi^*$) donor state following the photoexcitation of the carotenoid−porphyrin−C_{60} molecular triad solvated in tetrahydrofuran (THF) prepared in a geometry relaxed bent configuration in an optical cavity. The cavity frequency is changed in the ω_p = 200−400 meV range as indicated in the inset. The light−matter interaction strength is set at g_p = 20 meV. The temperature is set at T = 300 K. The calculations are based on TT-TFD simulations with a propagation time-step τ = 1 *au*.

under consideration at different values of ω_p (with the coupling strength g_p the same except for the cavity-free case, for which g_p = 0). The electron transfer rate is seen to be very sensitive to the value of ω_p, and the dependence of the electron transfer rate on ω_p is seen to be nonmonotonic. The effect of the cavity on the electron transfer dynamics is seen to be maximal when $\hbar\omega_p \sim$ 400 meV, which is consistent with previous estimates based on FGR according to which the resonance cavity frequency in this system is $\hbar\omega_p$ = 510 meV.[99]

Figure 4 compares the quantum-mechanically exact time evolution of the donor population obtained for model III in ref

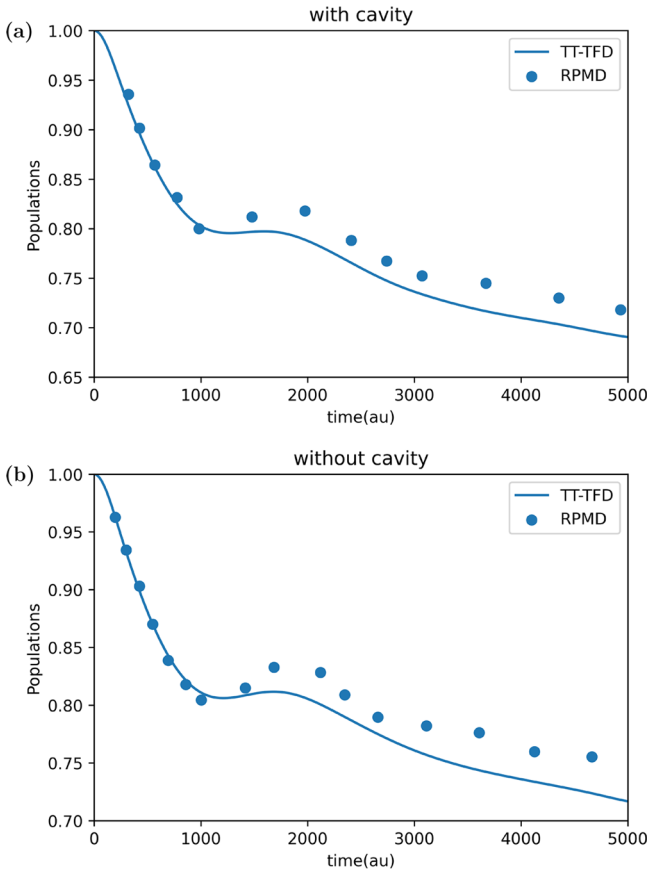

Figure 4. Comparison between population dynamics generated by TT-TFD and by RPMD for model III in ref 49. (a) Donor population with a cavity, (b) donor population without a cavity.

49 as obtained via the quantum-mechanically exact TT-TFD, to that obtained via the approximate ring-polymer molecular dynamics (RPMD) method (adopted from ref 49). While RPMD is seen to be rather accurate at short times, it is seen to be overdamped relative to the exact result and to lose accuracy at longer times.

Finally, Figure 5 compares the time evolution of the donor population in the carotenoid−porphyrin−C_{60}/THF system under consideration obtained via TT-TFD on a classical computer to that obtained via TT-TFD on a the IBM Osaka quantum computer. The results show that the quantum computing scheme is able to produce accurate results within about 1% error.

Results shown in Figures 2−5 indicate that the cavity lifetimes can be significant because it could affect reactions in the tens of femtoseconds. Our finding is consistent with the reported observations that the cavity can modify reaction rates on a wide range of time scales well beyond tens of femtoseconds, including reactions times as long as seconds to minutes.[23] These observations indicate that there is no direct relation between the time-scale of cavity losses and the time-scale of the rate processes impacted by placing the reacting chemical system inside the optical cavity.

To summarize, the modification of rates of chemical and physical processes via coupling to optical cavity modes is an area of significant current interest and promise. In this letter, we proposed a general-purpose quantum mechanically exact computational methodology for simulating cavity-modified electron transfer dynamics. The proposed method is based on

https://doi.org/10.1021/acs.jpclett.4c02220
J. Phys. Chem. Lett. 2024, 15, 9535−9542

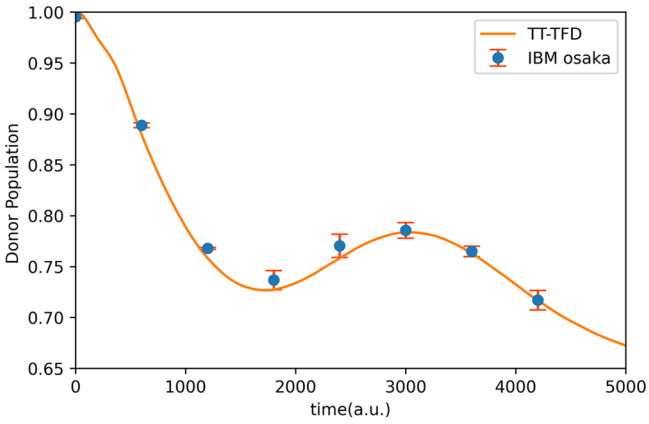

Figure 5. Time-dependent population of the ($\pi\pi^*$) state during the early time relaxation after photoexcitation of the carotenoid−porphyrin−C_{60} molecular triad solvated in tetrahydrofuran (THF) prepared in a geometry relaxed bent configuration in an optical cavity obtained with the IBM Osaka quantum computer. The cavity frequency is fixed at ω_p = 500 meV. The light−matter interaction strength is set at g_p = 20 meV. Matrix-free measurement mitigation is performed for readout error mitigation, as implemented in Qiskit. The blue dots are averages over 10 calculations following eq 18, each obtained with 2000 measurements. The error bar shows the highest and lowest values among the 10 runs.

TT-TFD, and extends its range of applicability from cavity-free systems to systems strongly coupled to an optical cavity. The accuracy and utility of the new approach was demonstrated on a model system parametrized to capture the essential physics underlying photoinduced electron transfer dynamics in the carotenoid−porphyrin−C_{60}/THF system. Significant enhancement of the electron transfer rate was found with increasing coupling between the molecular system and the cavity, as well a qualitative shift from overdamped monotonic decay dynamics to under-damped oscillatory dynamics. A strong nonmonotonic dependence of the electron transfer rate was also observed with respect to the cavity frequency, with the emergence of a resonance cavity frequency for which the effect of coupling to the cavity is maximal. Finally, we demonstrated how the TT-TFD electron transfer dynamics can be accurately simulated on NISQ computers.

We have demonstrated quantum computing simulations of electron transfer modulated by the effect of coupling to a polaritonic cavity mode, using a model lossless cavity employed by earlier studies, allowing for direct comparisons to recent RPMD simulations,[49] LSC-based methodologies[51] and studies based on Marcus theory.[99,100] These simulations on lossless cavities also allow for comparisons to an extended literature on polaritonic cavity models where the optical cavity is assumed to have a perfect internal reflectance and no loss of electromagnetic energy to the outside world.[59] The model is generic. It is not parametrized according to the experimental setup of a specific polaritonic cavity, and relies on a number of approximations that include restricting the model to two electronic states, assuming that the molecular system has no permanent dipole moment, and that is coupled to a single mode of a lossless cavity, while a typical experimental scenario might involve a weaker coupling to the cavity mode, or collective coupling of a large number of molecules to multiple modes of a lossy cavity, beyond the single molecule analysis. Work on extending the modeling beyond those restrictive approximations is currently underway and will be reported in forthcoming publications.

■ ASSOCIATED CONTENT

Data Availability Statement

The python code for the reported simulations is available at this link:https://github.com/NingyiLyu/Polaritonic_TT.

■ AUTHOR INFORMATION

Corresponding Authors

Victor S. Batista − *Department of Chemistry, Yale University, New Haven, Connecticut 06520, United States; Yale Quantum Institute, Yale University, New Haven, Connecticut 06511, United States;* orcid.org/0000-0002-3262-1237; Email: victor.batista@yale.edu

Eitan Geva − *Department of Chemistry, University of Michigan, Ann Arbor, Michigan 48109, United States;* orcid.org/0000-0002-7935-4586; Email: eitan@umich.edu

Authors

Ningyi Lyu − *Department of Chemistry, Yale University, New Haven, Connecticut 06520, United States; Multiscale Research Institute of Complex Systems, Fudan University, Shanghai 200433, China;* orcid.org/0000-0001-9239-9925

Pouya Khazaei − *Department of Chemistry, University of Michigan, Ann Arbor, Michigan 48109, United States*

Complete contact information is available at: https://pubs.acs.org/10.1021/acs.jpclett.4c02220

Notes

The authors declare no competing financial interest.

■ ACKNOWLEDGMENTS

The authors acknowledge support from the NSF grant 2124511 [CCI Phase I: NSF Center for Quantum Dynamics on Modular Quantum Devices (CQD-MQD)].

■ REFERENCES

(1) Tannor, D. J.; Rice, S. A. Coherent Pulse Sequence Control of Product Formation in Chemical Reactions. *Adv. Chem. Phys.* **1988**, *70*, 441−523.

(2) Kosloff, R.; Rice, S. A.; Gaspard, P.; Tersigni, S.; Tannor, D. J. Wave Packet Dancing: Achieving Chemical Selectivity By Shaping Light Pulses. *Chem. Phys.* **1989**, *139*, 201−220.

(3) Gordon, R. J.; Rice, S. A. Active Control of The Dynamics of Atoms and Molecules. *Annu. Rev. Phys. Chem.* **1997**, *48*, 601−641.

(4) Assion, A.; Baumert, T.; Bergt, M.; Brixner, T.; Kiefer, B.; Seyfried, V.; Strehle, M.; Gerber, G. Control of Chemical Reactions by Feedback-Optimized Phase-Shaped Femtosecond Laser Pulses. *Science* **1998**, *282*, 919−922.

(5) Rabitz, H.; Zhu, W. Optimal Control of Molecular Motion: Design Implementation and Inversion. *Acc. Chem. Res.* **2000**, *33*, 572−578.

(6) Rice, S. A.; Zhao, M. *Optical Control of Molecular Dynamics*; Wiley: New York, 2000.

(7) Levis, R. J.; Menkir, G. M.; Rabitz, H. Selective Bond Dissociation and Rearrangement With Optimally Tailored Strong Field Laser Pulses. *Science* **2001**, *292*, 709−713.

(8) Pearson, B. J.; White, J. L.; Weinacht, T. C.; Bucksbaum, P. H. Coherent Control Using Adaptive Learning Algorithms. *Phys. Rev. A* **2001**, *63*, 063412.

(9) Rice, S. A.; Shah, S. P. Active Control of Product Selection in A Chemical Reaction: A View of The Current Scene. *Phys. Chem. Chem. Phys.* **2002**, *4*, 1683−1700.
(10) Shapiro, M.; Brumer, P. *Principles of The Quantum Control of Molecular Processes*; Wiley: Hoboken, NJ, 2002.
(11) McRobbie, P.; Geva, E. Coherent Control of Population Transfer via Linear Chirp in Liquid Solution: The Role of Motional Narrowing. *J. Phys. Chem. A* **2016**, *120*, 3015−3022.
(12) Andrew, P.; Barnes, W. L. Förster energy transfer in an optical microcavity. *Science* **2000**, *290*, 785−788.
(13) Schwartz, T.; Hutchison, J.; Genet, C.; Ebbesen, T. Reversible Switching of Ultrastrong Light-Molecule Coupling. *Phys. Rev. Lett.* **2011**, *106*, 196405−4.
(14) Hutchison, J.; Schwartz, T.; Genet, C.; Devaux, E.; Ebbesen, T. Modifying Chemical Landscapes by Coupling to Vacuum Fields. *Angew. Chem. Int.* **2012**, *51*, 1592−1596.
(15) Hutchison, J.; Liscio, A.; Schwartz, T.; Canaguier-Durand, A.; Genet, C.; Palermo, V.; Samorì, P.; Ebbesen, T. Tuning the Work-Function Via Strong Coupling. *Adv. Mater.* **2013**, *25*, 2481−2485.
(16) Törmä, P.; Barnes, W. Strong coupling between surface plasmon polaritons and emitters: A review. *Rep. Prog. Phys.* **2015**, *78*, 013901−35.
(17) Flick, J.; Ruggenthaler, M.; Appel, H.; Rubio, A. Kohn−Sham approach to quantum electrodynamical density-functional theory: Exact time-dependent effective potentials in real space. *Proc. Natl. Acad. Sci. U.S.A.* **2015**, *112*, 15285−15290.
(18) Feist, J.; Garcia-Vidal, F. Extraordinary Exciton Conductance Induced by Strong Coupling. *Phys. Rev. Lett.* **2015**, *114*, 196402−5.
(19) Schachenmayer, J.; Genes, C.; Tignone, E.; Pupillo, G. Cavity-Enhanced Transport of Excitons. *Phys. Rev. Lett.* **2015**, *114*, 196403−6.
(20) Shalabney, A.; George, J.; Hutchison, J.; Pupillo, G.; Genet, C.; Ebbesen, T. Coherent coupling of molecular resonators with a microcavity mode. *Nat. Commun.* **2015**, *6*, 5981.
(21) Orgiu, E.; George, J.; Hutchison, J.; Devaux, E.; Dayen, J.; Doudin, B.; Stellacci, F.; Genet, C.; Schachenmayer, J.; Genes, C.; Pupillo, G.; Samorì, P.; Ebbesen, T. Conductivity in organic semiconductors hybridized with the vacuum field. *Nat. Mater.* **2015**, *14*, 1123−1129.
(22) Long, J.; Simpkins, B. Coherent Coupling between a Molecular Vibration and Fabry−Perot Optical Cavity to Give Hybridized States in the Strong Coupling Limit. *ACS Photonics* **2015**, *2*, 130−136.
(23) Ebbesen, T. Hybrid Light-Matter States in a Molecular and Material Science Perspective. *Acc. Chem. Res.* **2016**, *49*, 2403−2412.
(24) Thomas, A.; George, J.; Shalabney, A.; Dryzhakov, M.; Varma, S.; Moran, J.; Chervy, T.; Zhong, X.; Devaux, E.; Genet, C.; Hutchison, J.; Ebbesen, T. Ground-State Chemical Reactivity under Vibrational Coupling to the Vacuum Electromagnetic Field. *Angew. Chem.* **2016**, *128*, 11634−11638.
(25) Zhong, X.; Chervy, T.; Wang, S.; George, J.; Thomas, A.; Hutchison, J.; Devaux, E.; Genet, C.; Ebbesen, T. Non-Radiative Energy Transfer Mediated by Hybrid Light-Matter States. *Angew. Chem.* **2016**, *128*, 6310−6314.
(26) Herrera, F.; Spano, F. Cavity-Controlled Chemistry in Molecular Ensembles. *Phys. Rev. Lett.* **2016**, *116*, 238301−6.
(27) Casey, S.; Sparks, J. Vibrational Strong Coupling of Organometallic Complexes. *J. Phys. Chem. C* **2016**, *120*, 28138−28143.
(28) Sanvitto, D.; Kéna-Cohen, S. The road towards polaritonic devices. *Nat. Mater.* **2016**, *15*, 1061−1073.
(29) Kowalewski, M.; Bennett, K.; Mukamel, S. Cavity Femtochemistry: Manipulating Nonadiabatic Dynamics at Avoided Crossings. *J. Phys. Chem. Lett.* **2016**, *7*, 2050−2054.
(30) Kowalewski, M.; Bennett, K.; Mukamel, S. Non-adiabatic dynamics of molecules in optical cavities. *J. Chem. Phys.* **2016**, *144*, 054309.
(31) Flick, J.; Ruggenthaler, M.; Appel, H.; Rubio, A. Atoms and molecules in cavities, from weak to strong coupling in quantum-electrodynamics (QED) chemistry. *Proc. Natl. Acad. Sci. U.S.A.* **2017**, *114*, 3026−3034.
(32) Zhong, X.; Chervy, T.; Zhang, L.; Thomas, A.; George, J.; Genet, C.; Hutchison, J.; Ebbesen, T. Energy Transfer between Spatially Separated Entangled Molecules. *Angew. Chem., Int. Ed.* **2017**, *56*, 9034−9038.
(33) Martínez-Martínez, L.; Ribeiro, R.; Campos-González-Angulo, J.; Yuen-Zhou, J. Can Ultrastrong Coupling Change Ground-State Chemical Reactions? *ACS Photonics* **2018**, *5*, 167−176.
(34) Fregoni, J.; Granucci, G.; Coccia, E.; Persico, M.; Corni, S. Manipulating azobenzene photoisomerization through strong light-molecule coupling. *Nat. Commun.* **2018**, *9*, 4688.
(35) Sáez-Blázquez, R.; Feist, J.; Fernández-Domínguez, A.; García-Vidal, F. Organic polaritons enable local vibrations to drive long-range energy transfer. *Phys. Rev. B* **2018**, *97*, 241407−5.
(36) Flick, J.; Welakuh, D.; Ruggenthaler, M.; Appel, H.; Rubio, A. Light−Matter Response in Nonrelativistic Quantum Electrodynamics. *ACS Photonics* **2019**, *6*, 2757−2778.
(37) Galego, J.; Climent, C.; Garcia-Vidal, F.; Feist, J. Cavity Casimir-Polder Forces and Their Effects in Ground-State Chemical Reactivity. *Phys. Rev. X* **2019**, *9*, 021057−22.
(38) Lather, J.; Bhatt, P.; Thomas, A.; Ebbesen, T.; George, J. Cavity Catalysis by Cooperative Vibrational Strong Coupling of Reactant and Solvent Molecules. *Angew. Chem., Int. Ed.* **2019**, *58*, 10635−10638.
(39) Schäfer, C.; Ruggenthaler, M.; Appel, H.; Rubio, A. Modification of excitation and charge transfer in cavity quantum-electrodynamical chemistry. *Proc. Natl. Acad. Sci. U.S.A.* **2019**, *116*, 4883−4892.
(40) Hoffmann, N.; Schäfer, C.; Rubio, A.; Kelly, A.; Appel, H. Capturing vacuum fluctuations and photon correlations in cavity quantum electrodynamics with multitrajectory Ehrenfest dynamics. *Phys. Rev. A* **2019**, *99*, 063819−9.
(41) Hoffmann, N.; Schäfer, C.; Säkkinen, N.; Rubio, A.; Appel, H.; Kelly, A. Benchmarking semiclassical and perturbative methods for real-time simulations of cavity-bound emission and interference. *J. Chem. Phys.* **2019**, *151*, 244113.
(42) Lacombe, L.; Hoffmann, N.; Maitra, N. Exact Potential Energy Surface for Molecules in Cavities. *Phys. Rev. Lett.* **2019**, *123*, 083201−6.
(43) Mandal, A.; Huo, P. Investigating New Reactivities Enabled by Polariton Photochemistry. *J. Phys. Chem. Lett.* **2019**, *10*, 5519−5529.
(44) Semenov, A.; Nitzan, A. Electron transfer in confined electromagnetic fields. *J. Chem. Phys.* **2019**, *150*, 174122.
(45) Hoffmann, N.; Lacombe, L.; Rubio, A.; Maitra, N. Effect of many modes on self-polarization and photochemical suppression in cavities. *J. Chem. Phys.* **2020**, *153*, 104103.
(46) Flick, J.; Rivera, N.; Narang, P. Strong light-matter coupling in quantum chemistry and quantum photonics. *Nanophotonics* **2018**, *7*, 1479−1501.
(47) Gu, B.; Mukamel, S. Manipulating nonadiabatic conical intersection dynamics by optical cavities. *Chem. Sci.* **2020**, *11*, 1290−1298.
(48) Mandal, A.; Krauss, T.; Huo, P. Polariton-Mediated Electron Transfer via Cavity Quantum Electrodynamics. *J. Phys. Chem. B* **2020**, *124*, 6321−6340.
(49) Chowdhury, S.; Mandal, A.; Huo, P. Ring polymer quantization of the photon field in polariton chemistry. *J. Chem. Phys.* **2021**, *154*, 044109.
(50) Saller, M.; Kelly, A.; Geva, E. Benchmarking Quasiclassical Mapping Hamiltonian Methods for Simulating Cavity-Modified Molecular Dynamics. *J. Phys. Chem. Lett.* **2021**, *12*, 3163−3170.
(51) Saller, M. A. C.; Lai, Y.; Geva, E. An Accurate Linearized Semiclassical Approach for Calculating Cavity-Modified Charge Transfer Rate Constants. *J. Phys. Chem. Lett.* **2022**, *13*, 2330−2337.
(52) Basov, D.; Asenjo-Garcia, A.; Schuck, P.; Zhu, X.; Rubio, A. Polariton panorama. *Nanophotonics* **2020**, *10*, 549−577.
(53) Yuen-Zhou, J.; Xiong, W.; Shegai, T. Polariton chemistry: Molecules in cavities and plasmonic media. *J. Chem. Phys.* **2022**, *156*, 030401.

https://doi.org/10.1021/acs.jpclett.4c02220
J. Phys. Chem. Lett. 2024, 15, 9535−9542

(54) Li, T. E.; Nitzan, A.; Subotnik, J. E. Polariton relaxation under vibrational strong coupling: Comparing cavity molecular dynamics simulations against Fermi's golden rule rate. *J. Chem. Phys.* **2022**, *156*, 134106.
(55) Lindoy, L. P.; Mandal, A.; Reichman, D. R. Resonant Cavity Modification of Ground-State Chemical Kinetics. *J. Phys. Chem. Lett.* **2022**, *13*, 6580−6586.
(56) Cao, J. Generalized Resonance Energy Transfer Theory: Applications to Vibrational Energy Flow in Optical Cavities. *J. Phys. Chem. Lett.* **2022**, *13*, 10943−10951.
(57) Pavošević, F.; Smith, R. L.; Rubio, A. Cavity Click Chemistry: Cavity-Catalyzed Azide−Alkyne Cycloaddition. *J. Phys. Chem. A* **2023**, *127*, 10184−10188.
(58) Ying, W.; Taylor, M. A. D.; Huo, P. Resonance theory of vibrational polariton chemistry at the normal incidence. *Nanophotonics* **2024**, *13*, 2601−2615.
(59) Mandal, A.; Li, X.; Huo, P. Theory of vibrational polariton chemistry in the collective coupling regime. *J. Chem. Phys.* **2022**, *156*, 014101.
(60) Ying, W.; Huo, P. Resonance theory and quantum dynamics simulations of vibrational polariton chemistry. *J. Chem. Phys.* **2023**, *159*, 084104.
(61) Campos-Gonzalez-Angulo, J. A.; Poh, Y. R.; Du, M.; Yuen-Zhou, J. Swinging between shine and shadow: Theoretical advances on thermally activated vibropolaritonic chemistry. *J. Chem. Phys.* **2023**, *158*, 230901.
(62) Ahn, W.; Triana, J. F.; Recabal, F.; Herrera, F.; Simpkins, B. S. Modification of ground-state chemical reactivity via light−matter coherence in infrared cavities. *Science* **2023**, *380*, 1165−1168.
(63) Mandal, A.; Taylor, M. A.; Weight, B. M.; Koessler, E. R.; Li, X.; Huo, P. Theoretical Advances in Polariton Chemistry and Molecular Cavity Quantum Electrodynamics. *Chem. Rev.* **2023**, *123*, 9786−9879.
(64) Tibben, D. J.; Bonin, G. O.; Cho, I.; Lakhwani, G.; Hutchison, J.; Gómez, D. E. Molecular Energy Transfer under the Strong Light−Matter Interaction Regime. *Chem. Rev.* **2023**, *123*, 8044−8068.
(65) Hirai, K.; Hutchison, J. A.; Uji-i, H. Molecular Chemistry in Cavity Strong Coupling. *Chem. Rev.* **2023**, *123*, 8099−8126.
(66) Ruggenthaler, M.; Sidler, D.; Rubio, A. Understanding Polaritonic Chemistry from Ab Initio Quantum Electrodynamics. *Chem. Rev.* **2023**, *123*, 11191−11229.
(67) Bhuyan, R.; Mony, J.; Kotov, O.; Castellanos, G. W.; Gomez-Rivas, J.; Shegai, T. O.; Börjesson, K. The Rise and Current Status of Polaritonic Photochemistry and Photophysics. *Chem. Rev.* **2023**, *123*, 10877−10919.
(68) Xiang, B.; Xiong, W. Molecular Polaritons for Chemistry, Photonics and Quantum Technologies. *Chem. Rev.* **2024**, *124*, 2512−2552.
(69) Miller, W. H. Classical S-matrix: Numerical application to inelastic collisions. *J. Chem. Phys.* **1970**, *53*, 3578.
(70) Meyer, H.-D.; Miller, W. H. A classical analog for electronic degrees of freedom in nonadiabatic collision processes. *J. Chem. Phys.* **1979**, *70*, 3214−3223.
(71) Stock, G.; Thoss, M. Semiclassical Description of Nonadiabatic Quantum Dynamics. *Phys. Rev. Lett.* **1997**, *78*, 578−581.
(72) Miller, W. The semiclassical initial value representation: A potentially practical way for adding quantum effects to classical molecular dynamics simulations. *J. Phys. Chem. A* **2001**, *105*, 2942−2955.
(73) Wang, H.; Sun, X.; Miller, W. H. Semiclassical approximations for the calculation of thermal rate constants for chemical reactions in complex molecular systems. *J. Chem. Phys.* **1998**, *108*, 9726.
(74) Coronado, E. A.; Xing, J.; Miller, W. H. Ultrafast non-adiabatic dynamics of systems with multiple surface crossing: A test of the Meyer-Miller Hamiltonian with semiclassical initial value representation methods. *Chem. Phys. Lett.* **2001**, *349*, 521.
(75) Cotton, S. J.; Miller, W. H. Symmetrical windowing for quantum states in quasi-classical trajectory simulations: Application to electronically non-adiabatic processes. *J. Chem. Phys.* **2013**, *139*, 234112.
(76) Cotton, S.; Miller, W. The Symmetrical Quasi-Classical Model for Electronically Non-Adiabatic Processes Applied to Energy Transfer Dynamics in Site-Exciton Models of Light-Harvesting Complexes. *J. Chem. Theory Comput.* **2016**, *12*, 983−991.
(77) Saller, M.; Kelly, A.; Richardson, J. On the identity of the identity operator in nonadiabatic linearized semiclassical dynamics. *J. Chem. Phys.* **2019**, *150*, 071101.
(78) Makri, N.; Miller, W. H. Monte carlo integration with oscillatory integrands: implications for feynman path integration in real time. *Chem. Phys. Lett.* **1987**, *139*, 10.
(79) Makri, N. Improved Feynman propagators on a grid and nonadiabatic corrections within the path integral framework. *Chem. Phys. Lett.* **1992**, *193*, 435.
(80) Yan, Y.; Xu, M.; Li, T.; Shi, Q. Efficient propagation of the hierarchical equations of motion using the Tucker and hierarchical Tucker tensors. *J. Chem. Phys.* **2021**, *154*, 194104.
(81) Oseledets, I.; Tyrtyshnikov, E. TT-cross approximation for multidimensional arrays. *Linear Algebra and Its Applications* **2010**, *432*, 70−88.
(82) Oseledets, I. V. Tensor-train decomposition. *SIAM Journal on Scientific Computing* **2011**, *33*, 2295−2317.
(83) Lyu, N.; Soley, M. B.; Batista, V. S. Tensor-Train Split-Operator KSL (TT-SOKSL) Method for Quantum Dynamics Simulations. *J. Chem. Theory Comput.* **2022**, *18*, 3327−3346.
(84) Preskill, J. Quantum computing in the NISQ era and beyond. *Quantum* **2018**, *2*, 79.
(85) Shen, Y.; Lu, Y.; Zhang, K.; Zhang, J.; Zhang, S.; Huh, J.; Kim, K. Quantum optical emulation of molecular vibronic spectroscopy using a trapped-ion device. *Chemical Science* **2018**, *9*, 836−840.
(86) Hempel, C.; Maier, C.; Romero, J.; McClean, J.; Monz, T.; Shen, H.; Jurcevic, P.; Lanyon, B. P.; Love, P.; Babbush, R.; Aspuru-Guzik, A.; Blatt, R.; Roos, C. F. Quantum Chemistry Calculations on a Trapped-Ion Quantum Simulator. *Physical Review X* **2018**, *8*, 031022.
(87) Du, J.; Xu, N.; Peng, X.; Wang, P.; Wu, S.; Lu, D. NMR Implementation of a Molecular Hydrogen Quantum Simulation with Adiabatic State Preparation. *Phys. Rev. Lett.* **2010**, *104*, 030502.
(88) Colless, J.; Ramasesh, V.; Dahlen, D.; Blok, M.; Kimchi-Schwartz, M.; McClean, J.; Carter, J.; de Jong, W.; Siddiqi, I. Computation of Molecular Spectra on a Quantum Processor with an Error-Resilient Algorithm. *Physical Review X* **2018**, *8*, 011021.
(89) Kananenka, A.; Sun, X.; Schubert, A.; Dunietz, B.; Geva, E. A comparative study of different methods for calculating electronic transition rates. *J. Chem. Phys.* **2018**, *148*, 102304.
(90) Sajjan, M.; Li, J.; Selvarajan, R.; Sureshbabu, S. H.; Kale, S. S.; Gupta, R.; Singh, V.; Kais, S. Quantum machine learning for chemistry and physics. *Chem. Soc. Rev.* **2022**, *51*, 6475−6573.
(91) Borrelli, R.; Gelin, M. F. Finite temperature quantum dynamics of complex systems: Integrating thermo-field theories and tensor-train methods. *Wiley Interdisciplinary Reviews: Computational Molecular Science* **2021**, *11*, No. e1539.
(92) Lyu, N.; Mulvihill, E.; Soley, M. B.; Geva, E.; Batista, V. S. Tensor-Train Thermo-Field Memory Kernels for Generalized Quantum Master Equations. *J. Chem. Theory Comput.* **2023**, *19*, 1111−1129.
(93) Wang, Y.; Mulvihill, E.; Hu, Z.; Lyu, N.; Shivpuje, S.; Liu, Y.; Soley, M. B.; Geva, E.; Batista, V. S.; Kais, S. Simulating Open Quantum System Dynamics on NISQ Computers with Generalized Quantum Master Equations. *J. Chem. Theory Comput.* **2023**, *19*, 4851−4862.
(94) Nagy, B. S.; Foias, C. *Harmonic Analysis of Operators on Hilbert Space*; Holland Publishing Co.: Amsterdam, London, 1970.
(95) Hu, Z.; Xia, R.; Kais, S. A quantum algorithm for evolving open quantum dynamics on quantum computing devices. *Sci. Rep.* **2020**, *10*, 3301.
(96) Schlimgen, A. W.; Head-Marsden, K.; Sager, L. M.; Narang, P.; Mazziotti, D. A. Quantum simulation of open quantum systems using

https://doi.org/10.1021/acs.jpclett.4c02220
J. Phys. Chem. Lett. 2024, 15, 9535−9542

a unitary decomposition of operators. *Phys. Rev. Lett.* **2021**, *127*, 270503.
(97) Hu, Z.; Head-Marsden, K.; Mazziotti, D. A.; Narang, P.; Kais, S. A general quantum algorithm for open quantum dynamics demonstrated with the Fenna-Matthews-Olson complex. *Quantum* **2022**, *6*, 726.
(98) Chowdhury, S. N.; Huo, P. Coherent state mapping ring polymer molecular dynamics for non-adiabatic quantum propagations. *J. Chem. Phys.* **2017**, *147*, 214109.
(99) Saller, M. A. C.; Lai, Y.; Geva, E. Cavity-Modified Fermi's Golden Rule Rate Constants from Cavity-Free Inputs. *J. Phys. Chem. C* **2023**, *127*, 3154−3164.
(100) Saller, M. A. C.; Lai, Y.; Geva, E. Cavity-modified Fermi's golden rule rate constants: beyond the single mode approximation. *J. Chem. Phys.* **2023**, *159*, 151105.
(101) Weidman, J. D.; Dadgar, M. S.; Stewart, Z. J.; Peyton, B. G.; Ulusoy, I. S.; Wilson, A. K. Cavity-modified molecular dipole switching dynamics. *J. Chem. Phys.* **2024**, *160*, 094111.
(102) Sun, X.; Zhang, P.; Lai, Y.; Williams, K.; Cheung, M.; Dunietz, B.; Geva, E. Computational Study of Charge-Transfer Dynamics in the Carotenoid-Porphyrin-C_{60} Molecular Triad Solvated in Explicit Tetrahydrofuran and Its Spectroscopic Signature. *J. Phys. Chem. C* **2018**, *122*, 11288−11299.
(103) Tong, Z.; Gao, X.; Cheung, M.; Dunietz, B.; Geva, E.; Sun, X. Charge transfer rate constants for the carotenoid-porphyrin-C_{60} molecular triad dissolved in tetrahydrofuran: The spin-boson model vs the linearized semiclassical approximation. *J. Chem. Phys.* **2020**, *153*, 044105.
(104) Lyu, N.; Miano, A.; Tsioutsios, I.; Cortiñas, R. G.; Jung, K.; Wang, Y.; Hu, Z.; Geva, E.; Kais, S.; Batista, V. S. Mapping Molecular Hamiltonians into Hamiltonians of Modular cQED Processors. *J. Chem. Theory Comput.* **2023**, *19*, 6564−6576.
(105) Levy, E.; Shalit, O. M. Dilation theory in finite dimensions: the possible, the impossible and the unknown. *Rocky Mt. J. Math.* **2014**, *44*, 203−221.

https://doi.org/10.1021/acs.jpclett.4c02220
J. Phys. Chem. Lett. 2024, 15, 9535−9542